

Performance of piezoelectric semiconductor bipolar junction transistors and the tuning mechanism by mechanical loadings

Cite as: J. Appl. Phys. 133, 145701 (2023); doi: 10.1063/5.0141524

Submitted: 6 January 2023 · Accepted: 22 March 2023 ·

Published Online: 11 April 2023



View Online



Export Citation



CrossMark

Yizhan Yang,¹ Wanli Yang,¹ Yunbo Wang,² Xiangbin Zeng,² and Yuantai Hu^{1,a)}

AFFILIATIONS

¹ Department of Mechanics, School of Aerospace Engineering, Hubei Key Laboratory of Engineering Structural Analysis and Safety Assessment, Huazhong University of Science and Technology, Wuhan 430074, China

² Department of Microelectronics, School of Optical and Electronic Information, Huazhong University of Science and Technology, Wuhan 430074, China

^{a)}Author to whom correspondence should be addressed: hudeng@263.net

ABSTRACT

A coupling model is established on piezoelectric semiconductor bipolar junction transistors (PS-BJT) subjected to mechanical loadings by abandoning depletion layer approximation and low injection assumption. Effect of base region on device performance and interaction between emitter/base junction (E/B) and base/collector junction (B/C) are investigated. It is found that too small a base width will cause B/C to extract electrons directly from emitter region, implying that an electron passageway will be excited to link from collector- to emitter-region by striding over base-region (abbreviated as “EP-CE” hereafter). We particularly clarify that the current produced by electrons flowing across EP-CE is independent of electron-hole recombination in E/B, which means that this current has not yet been bestowed on the information of base current. “Information of base current” refers to dispatching information of base current on the electrons in emitter region. Thus, a current from EP-EC cannot be reckoned in the amplification effect of base current. Our investigations show that base width should not be designed too small to avoid EP-CE, which has not been revealed before. As regards to tuning PS-BJT performance by mechanical loadings, we revealed the mechanism as follows: 1) raising electron-hole recombination rate inside E/B to reduce resistivity such that more electrons can be driven from emitter- to base-region; 2) elevating electron conductivity in base-region for easier pass of electrons; 3) promoting attractive ability of B/C on electrons such that more electrons cross the interface. Numerical results show that transmission characteristics can be greatly increased as expected by mechanical tuning.

Published under an exclusive license by AIP Publishing. <https://doi.org/10.1063/5.0141524>

Downloaded from http://pubs.aip.org/aip/jap/article-pdf/doi/10.1063/5.0141524/16824610/145701_1_5.0141524.pdf

I. INTRODUCTION

Piezoelectric semiconductors (PSs) have important applications in electronic devices due to their coupling characteristics of piezoelectricity and semiconductor. Interaction between electromechanical coupling fields and charge carriers enables PS structures able to implement the function of mutual conversion between mechanical energy and electrical energy or mechanical signal and electrical signal. Thus, PS structures have been often used in recent decades to make nanogenerators,^{1–3} field effect transistors,^{4,5} high-sensitivity strain sensors,^{6,7} optoelectronic devices,^{8,9} acoustic wave amplifiers,^{10,11} and so on. Moreover, because the deformations

induced polarization electric field in PS structures will drive charge carriers into redistribution, and carrier redistribution will produce shielding effect on electric field itself in turn, mechanical tuning on the performance of PS devices has become an actual hot issue at present, too. Thus, reforming the configuration of a potential barrier near an interface inside PS devices via an artificial potential barrier induced by mechanical loadings can produce regulation action on the transport process of charge carriers,¹² and further realize effective control on the behavior of microelectronic devices, such as PN junctions,^{13–16} quantum wells,^{17,18} and quantum dots.¹⁹ Obviously, it is necessary to open the interface barrier to fully understand the change characteristics of its internal physical

quantities. Thus, it is specially required to establish a coupled model on the interaction of electromechanical coupling fields and charge carriers to promote the applications and developments of PS devices. Luo *et al.*²⁰ developed an analytical model on piezoelectric semiconductor PN junctions and studied the change laws of interface electrical characteristics when subjected to mechanical loadings. Yang *et al.*¹⁴ established an analytical model on gradient doped PN junctions and found that when tuning PS devices mechanically, the self-built electric field generated by the doping gradient will partly shield the polarization electric field. In addition, Yang *et al.*¹⁵ also studied the PN junction in a PS composite structure and obtained some helpful results in the designs of mechanical tuning on the performance of piezoelectric devices. Furthermore, Yang *et al.*²¹ found the sensitivity of PS composite structures to the ambient temperature increment and studied the effect of temperature increment on structure performance. Fan *et al.*²² studied performance of a piecewise-stressed ZnO nanofiber with the multi-field coupling theory and found specific distributions of potential barriers and wells produced by equal and opposite forces. Huang *et al.*²³ studied the mechanical tuning effect on the characteristics of PS structures and obtained some useful results afterwards. However, it should be noted that the above studies have introduced a linearization assumption on drift current for simplicity, which is improper to be extended to analysis on the interface potential barrier in the PN junction. As well known, electric potential, electric field, and carrier concentrations present upheaval change in the barrier region of PN junctions. It is precisely such dramatic change physical process in the interface region to be pregnant with a series of new physical phenomena which are the basis for further development of modern microelectronic devices. Thereupon, studying and tuning on the nature of piezoelectric PN junctions via mechanical loadings can give some promotional effect on designing and developing modern functions of piezotronic devices. Yang *et al.*²⁴ put forward a full-coupling model on a PN junction by fully opening the barrier area of a PN junction. Majority-carrier current was exactly defined and mutual conversion between majority- and minority-carrier currents was shown inside the whole PN junction region. Further, Yang *et al.*²⁵ and Yang *et al.*²⁶ used the fully-coupled model to analyze the characteristics of PN junctions with the piezo-effect. The regulation mechanism of mechanical loadings on performance of PN junctions was clarified in detail in Ref. 25

and an artificial barrier method was put forward finally.²⁶ Specific to bipolar junction transistors (BJTs), there exist two PN junctions in each bipolar junction transistor and the interaction between two junctions implement the amplification function of base current. In the classical semiconductor framework, the approximation of depletion layer and assumption of low injection are applied for simplicity.^{27,28} Obviously, there exist the following limitations from the above approximation and assumption to analyze BJT performance: (1) the mutual conversion process of majority- and minority-carrier currents at E/B interface neither be definitely displayed, nor can the information conversion from hole current to electron current be clearly presented, nor can the mechanism of mechanical regulation on BJT performance be revealed; (2) it is difficult to quantitatively investigate the effect of base width on BJT performance and then to design its proper width; (3) it is not conducive to design the effective method to strengthen the attraction of the B/C junction on electrons; (4) it is not suitable for analyzing BJT characteristics under large injection. Although Zhu *et al.*⁶ studied changes in the electrical characteristics of a PS-BJT under tensile/compressive strains and found that PS transistors are sensitive to deformations, regulating mechanism of mechanical loadings on the transmission characteristics of PS-BJT are still needed further investigation.

In this paper, a coupling model on an npn-type PS-BJT is built at first. Then, attention is paid on the characteristics of energy levels of a PS-BJT under thermal equilibrium state and the effect of base width on device performance. Following, mechanical tuning mechanism on input-, output-, and transmission-characteristics of a PS-BJT is clarified in detail. Finally, it is found that mechanical tuning on a PS-BJT should be focused on the resistivity at E/B junction, the attractive ability of B/C junction on the base electrons, and the electron conductivity in the base region.

II. COUPLING MODELING ON PIEZOELECTRIC SEMICONDUCTOR BIPOLAR JUNCTION TRANSISTORS SUBJECTED TO MECHANICAL LOADINGS

Figure 1(a) schematically exhibits the geometric configuration of a PS-BJT, where only half of the transistor along the x_2 -direction is shown due to symmetry relative to the x_1-x_3 plane at $x_2=0$. There exist two interfaces inside the transistor, i.e., an emitter

Downloaded from http://pubs.aip.org/aip/jap/article-pdf/doi/10.1063/5.0141524/16824610/145701_1_5.0141524.pdf

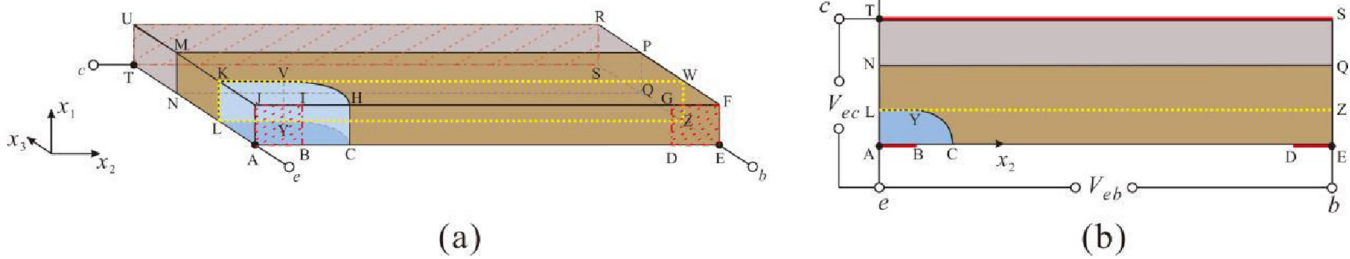


FIG. 1. Geometric configuration of a PS-BJT. (a) The 3D schematic diagram and (b) the sectional drawing at the x_2-x_3 plane.

interface KLYCHV between the emitter and base region (E/B junction) and a collector interface MNQP between the base and collector region (B/C junction).

Take an npn-typed transistor as the example. Doping in the PS-BJT is as follows: the blue gray emitter region with n-type heavy doping ($N_D^+ = 1 \times 10^{23} \text{ m}^{-3}$), the dark yellow base region with p-type light doping ($N_A = 1 \times 10^{21} \text{ m}^{-3}$), and the bright gray collector region with n-type doping ($N_D = 1 \times 10^{21} \text{ m}^{-3}$). Three electrodes are laid inside the red dashed borders JABI (emitter electrode), GDEF (base electrode), and UTSR (collector electrode) with three lead-wires out from them, respectively, marked as *e*, *b*, and *c*. Mechanically, the whole surface of the PS-BJT is stress free. Electrically, normal components of electric displacement and current are assumed vanishing in the non-electrode areas, while the Ohm contact conditions are applied in the electrode areas. Besides, the continuity conditions are assumed at the two junction interfaces: mechanical displacements and normal electric displacement, electric potential, majority- and minority-carrier currents. A plane profile of the PS-BJT with a common-emitter is shown in Fig. 1(b) for convenience in the later analyses, where the electric potential difference is denoted as V_{eb} between base- and emitter-electrodes and V_{ec} between collector- and emitter-electrodes. The dimension parameters of the PS-BJT and the corresponding value-ranges used in the following calculations are given in Table I.

The material is transversely isotropic with the *c* axis along the x_3 -direction. A pair of static stresses (σ) is loaded at KWZL-plane and MPQN-plane. Gauss's law and the current continuity equations, respectively, are

$$\begin{aligned} D_{i,i} &= q(p - n + N_D - N_A), \\ J_{i,i}^P &= -R, \quad J_{i,i}^n = R, \end{aligned} \quad (1)$$

where D_i stands for the electric displacement, n and p for electron and hole concentrations, respectively. $q = 1.6 \times 10^{-19} \text{ C}$ denotes the elementary charge. R denotes the recombination rate of carriers. We note that N_D in (1) should be written as N_D^+ when applied in the emitter region. J_i^n and J_i^P stand for electron and hole current

TABLE I. The dimension parameters of a PS-BJT and the corresponding value-ranges.

Geometric parameters	Implication
$L(\text{AE})$	The length of the transistor ($40 \mu\text{m}$)
$w(\text{AT})$	The width of the transistor ($4.0 \mu\text{m}$)
$h(\text{AJ})$	The height of the transistor
r	Curvature radius of the quarter arc HI ($0.5 \mu\text{m}$)
$d_e(\text{AL})$	The width of the emitter region ($0.5 \mu\text{m}$)
$d_b(\text{LN})$	The width of the base region ($1.0\text{--}2.0 \mu\text{m}$)
$d_c(\text{NT})$	The width of the collector region ($1.5\text{--}2.5 \mu\text{m}$)
$w_e(\text{AB})$	The width of the emitter electrode ($0.5 \mu\text{m}$)
$w_b(\text{DE})$	The width of the base electrode ($0.5 \mu\text{m}$)
$w_c(\text{TS} = \text{AE})$	The width of the collector electrode ($40 \mu\text{m}$)

densities, respectively, which can be expressed as

$$J_i^n = qn\mu_{ij}^n E_j + qD_{ij}^n n_j, \quad J_i^P = qp\mu_{ij}^P E_j - qD_{ij}^P p_j, \quad (2)$$

in which $\mu_{ij}^{(n,p)}$ and $D_{ij}^{(n,p)}$ represent the mobility and diffusion coefficients of electrons and holes, respectively, with the Einstein relationship $\mu_{ij}^{(n,p)} = D_{ij}^{(n,p)}kT/q$. Obviously, the component of electric displacement in the x_1 axis can be set null, $D_1 = 0$, while $D_{(2,3)} = (\bar{\epsilon}_{22}, \bar{\epsilon}_{33})E_{(2,3)} + (0, \hat{\epsilon}_{33}/\hat{\epsilon}_{33})\sigma$ with σ being external applied stress and $\bar{\epsilon}_{(22,33)} = (1 + \xi_{(22,33)}^2)\hat{\epsilon}_{(11,33)}$ referred to Ref. 29 $\xi_{22}^2 = e_{15}^2/(c_{44}\hat{\epsilon}_{11})$ and $\xi_{33}^2 = \hat{\epsilon}_{33}^2/(\hat{c}_{33}\hat{\epsilon}_{33})$ stand for the electromechanical coupling coefficients. In the above, stress release has been conducted in the x_1 -direction to obtain those modified coefficients as $(\hat{c}_{33}, \hat{\epsilon}_{33}) = (c_{33}, e_{33}) - 2(c_{13}, e_{31})c_{13}/(c_{11} + c_{12})$, $\hat{\epsilon}_{11} = \epsilon_{11}$, $\hat{\epsilon}_{33} = \epsilon_{33} + 2e_{31}^2/(c_{11} + c_{12})$.

The current continuity equations for electrons/holes in the PS-BJT are^{26,27}

$$\begin{aligned} \mu_{kj}^P p \phi_{jk} + \mu_{kj}^P p_j \phi_j + D_{kj}^P p_{jk} - R &= 0, \\ -\mu_{kj}^n n \phi_{jk} - \mu_{kj}^n n_j \phi_j + D_{kj}^n n_{jk} - R &= 0, \end{aligned} \quad (3)$$

where ϕ is the electric potential; R can be written as follows from the Shockley–Read–Hall recombination model,^{26,27}

$$R = \frac{np - n_i^2}{\tau_p(n + n_i) + \tau_n(p + n_i)}, \quad (4)$$

where τ_p and τ_n represent the lifetime of holes and electrons, respectively, and n_i is the intrinsic carrier concentration of piezoelectric semiconductors. When doping is completely ionized, the initial majority-carrier concentrations in every regions can be written as $(n_{e0}, p_{b0}, n_{c0}) = (N_D^+, N_A, N_D)$. Letting V_{eb}^0 be the contact electric potential difference between emitter- and base-electrodes, V_{ec}^0 the one between emitter- and collector-electrodes, respectively, we have

$$\begin{aligned} V_{eb}^0 &= -2.3(kT/q) \log(N_D^+ N_A / n_i^2); \\ V_{bc}^0 &= 2.3(kT/q) \log(N_D N_A / n_i^2). \end{aligned} \quad (5)$$

In addition, taking l_{eb} and l_{ec} as the potential barrier widths of the emitter junction and the collector junction, respectively, yields from²⁸

$$\begin{aligned} l_{eb} &= \sqrt{2\bar{\epsilon}_{33}|V_{eb}^0|(N_D^+ + N_A)/(qN_D^+ N_A)}; \\ l_{bc} &= \sqrt{2\bar{\epsilon}_{33}V_{bc}^0(N_D + N_A)/(qN_D N_A)}. \end{aligned} \quad (6)$$

III. THE CHARACTERISTICS OF ENERGY LEVELS OF A PS-BJT UNDER A THERMAL EQUILIBRIUM STATE AND THE FUNCTION OF THE BASE REGION ON DEVICE PERFORMANCE

There usually exist two PN junctions in a BJT, an E/B junction and a B/C junction. Doping in the emitter region is much heavier

than in the base region such that the potential barrier at the E/B interface lies almost totally inside the base region, while same doping in the base and collector region results in the potential barrier at the B/C interface to be located inside two equal zones at both sides of the junction. We note that two junctions are under different operation modes: (1) the E/B interface (equivalent to a sluice gate of electron flow) is opened by base voltage V_{eb} such that the electrons in the emitter region can be driven into the base region via diffusion. It should be noted that it is just in such a diffusion process that the information of hole current has been adhered to electron current via the electron-hole recombination or the inter-conversion between majority- and minority-carrier currents; (2) the electrons in the base region is pumped to the collector region by the collector voltage V_{ec} . We note that V_{ec} should be set as the one to take electrons as much as possible from the base region.

Difference between the above two operation modes indicates that V_{eb} and V_{ec} should attend to each one's own duties: V_{eb} plays the role to open the E/B interface and V_{ec} plays the role to pump electrons across the B/C interface. Mutual interference is negative to promote the device performance. Particularly, interference of V_{ec} on the operation mode of V_{eb} is unallowable, which implies that

V_{ec} cannot be set too large for a given V_{eb} . Otherwise, a directly coupling between two junctions without intermediate connect of the base region will be excited by V_{ec} . Under that case, an electronic passageway (EP-EC) with striding over the base region will be directly linked up from the collector region to the emitter region such that V_{ec} can directly catch electrons from the emitter region to the collector region. Obviously, electron flow through an EP-EC does not include the information of hole current because the information transfer from hole current to electron current is finished through the electron-hole recombination in the E/B junction, or say, the information transfer is reached via the inter-transformation of majority- and minority-carrier currents at the E/B junction. Furthermore, the higher the recombination rate, the lower the resistivity, and the more evident the amplification effect on information transfer from hole current to electron current. As regards the further transmission of the amplified current information from the base region to the collector region, it is required to improve the pumping capacity of the B/C junction on the base electrons and to increase the transport efficiency of electrons in the base region. We note that the pumping capacity refers to the incremental electric field in the B/C junction and the transport efficiency is related

Downloaded from http://pubs.aip.org/aip/jap/article-pdf/doi/10.1063/5.0141524/16824610/145701_1_5.0141524.pdf

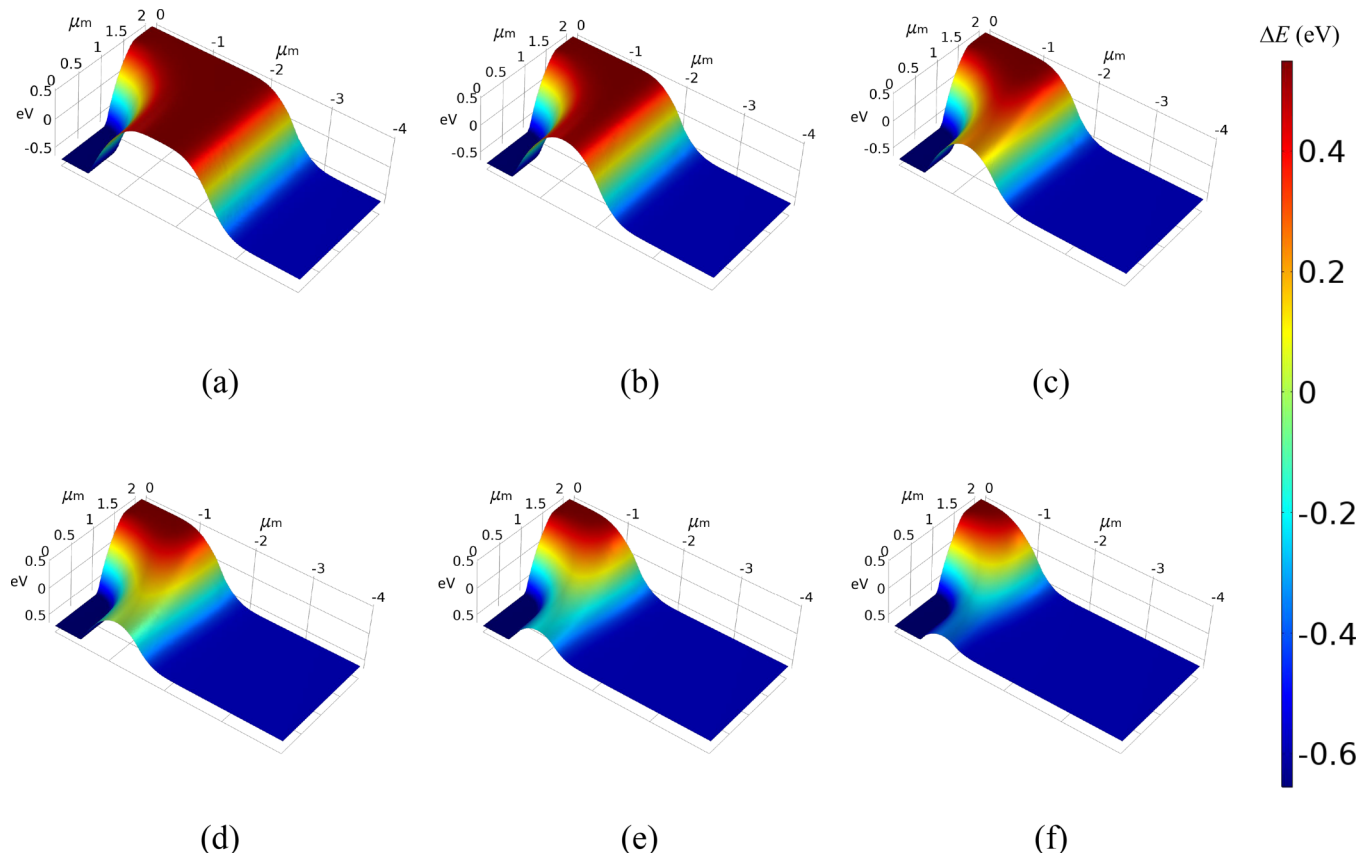


FIG. 2. Energy level difference inside a PS-BJT when d_b narrowing from 2.0 to 0.6 μm (a) $d_b = 2.0 \mu\text{m}$, (b) $d_b = 1.5 \mu\text{m}$, (c) $d_b = 1.2 \mu\text{m}$, (d) $d_b = 1.0 \mu\text{m}$, (e) $d_b = 0.8 \mu\text{m}$, and (f) $d_b = 0.6 \mu\text{m}$.

to the electron conductivity in the base region. Thus, the above analysis indicates that the width of the base region cannot be designed too small or too large, a too small d_b will induce the appearance of an EP-CE while those electrons through EP-CE are not able to embody the information of base current; and a too large d_b will cause weakening on the pumping capacity of the B/C junction and the transport efficiency in the base region.

In order to numerically clarify the effect of the base width on EP-CE, Fig. 2 shows the energy level difference $\Delta E = E_i - E_f$ of a PS-BJT under the thermal equilibrium when the base width becomes narrow from 2.0 to 0.6 μm . Interaction between two potential barriers at E/B and B/C junctions can be observed from Fig. 2. Considering that ZnO is with the largest electromechanical coupling coefficient in the third generation semiconductors, it is taken as the example material in the analyses for convenience in regulation on BJT performance, where the c axis is set in the x_3 -direction with the parameters obtained from^{21,28} as follows:

$$\begin{aligned} c_{11} &= 209 \text{ GPa}, \quad c_{12} = 120 \text{ GPa}, \quad c_{13} = 104 \text{ GPa}, \\ c_{33} &= 218 \text{ GPa}, \quad c_{44} = 44.1 \text{ GPa}; \quad e_{31} = -0.57 \text{ C m}^{-2}, \\ e_{33} &= 1.32 \text{ C m}^{-2}, \quad e_{15} = -0.48 \text{ C m}^{-2}; \quad \epsilon_{11} = 7.77 \epsilon_0, \\ \epsilon_{33} &= 8.91 \epsilon_0; \quad \mu_n = 0.0205 \text{ m}^2/\text{Vs}, \quad \mu_p = 0.007 \text{ m}^2/\text{Vs}, \\ \tau_n = \tau_p &= 1 \times 10^{-6} \text{ s}, \quad n_i = 1 \times 10^{12} \text{ m}^{-3}. \end{aligned} \quad (7)$$

When d_b is set relatively wide, for example, $d_b > 1.5 \mu\text{m}$, two barriers are clearly separated by the base region such that an EP-CE cannot appear. Thus, collector current I_c does completely come from the amplification information of base current I_b . However, as d_b gradually becomes narrow, two barrier zones start to join hands each other at the central base region, for example, $d_b < 1.2 \mu\text{m}$ as shown in Fig. 2. Under this situation, the barrier height near the KLMN-plane will be significantly reduced such that an EP-CE gradually becomes visible after $d_b < 1.2 \mu\text{m}$. Appearance of an EP-CE implies that a lot of electrons in the emitter region can be directly caught by V_{ce} to the collector region by striding over the base region, which induces part of collector current I_c not to come from the amplification effect of base current I_b . Thus, the size of the base region should neither be designed large on the one hand to prevent too many electrons to be recombined

by holes outside the E/B junction, nor can d_b be set too small on the other hand to avoid appearance of an EP-CE.

Figure 3 shows carrier distributions on the cross section AJUT under different base widths when subjected to different pairs of static stresses loaded at the KWZL-plane and MPQN-plane, where $(\bar{n}, \bar{p}) = (\log(n/n_i), \log(p/n_i))$. We note that although the regulation effect of mechanical loadings at the location adjacent to the E/B interface is relatively weak due to the strong shielding effect of high doping in the emitter region, the loading location with a tiny departure upward from the KWZL-plane presents evident tuning effect. When the base width is relatively large, for example, $d_b = 1.5 \mu\text{m}$ as shown in Fig. 3(a), two potential barrier zones are totally separated by the base region. Thus, the incremental electric field induced by a pair of tensile stresses ($\sigma > 0$) will drive the majority carriers from two sides into the E/B junction such that its barrier zone becomes narrow, while the majority carriers are driven out from the B/C junction by applied tensile stresses such that the barrier zone there becomes wide. Conversely, a pair of compressive stresses ($\sigma < 0$) enforces the E/B barrier zone to become wide and the B/C barrier zone to become narrow. As a result, regulation of $\sigma > 0 (< 0)$ makes two carrier concentrations approach one another (stay far away from each other) in the E/B junction, which implies rise (reduction) in the recombination rate and reduction (rise) in resistivity there. In the base region and B/C junction, regulation of $\sigma > 0 (< 0)$ makes electron concentration rise (reduce), implying rise (reduction) in the electron conductivity there. As the base width becomes small, two barrier regions begin to overlap, for example, when $d_b = 1.0 \mu\text{m}$, the B/C junction barrier partly superimpose on the emitter junction barrier gradually from top to bottom. The electric potential field caused by the B/C junction barrier elevates electronic potential energy in the overlapping zone to result in that holes are no longer majority carriers there, such as the case shown in Fig. 3(b) at the cross section AJUT sandwiched between the two interfaces. Under that situation, two concentrations of majority- and minority-carriers are close to each other. Thus, mechanical loadings produce less obvious effect on elevating the recombination rate and reducing the resistivity at the E/B interface as shown in Fig. 3(b). When the base width becomes smaller, the overlapping domain is further expanded and the electronic potential energy is

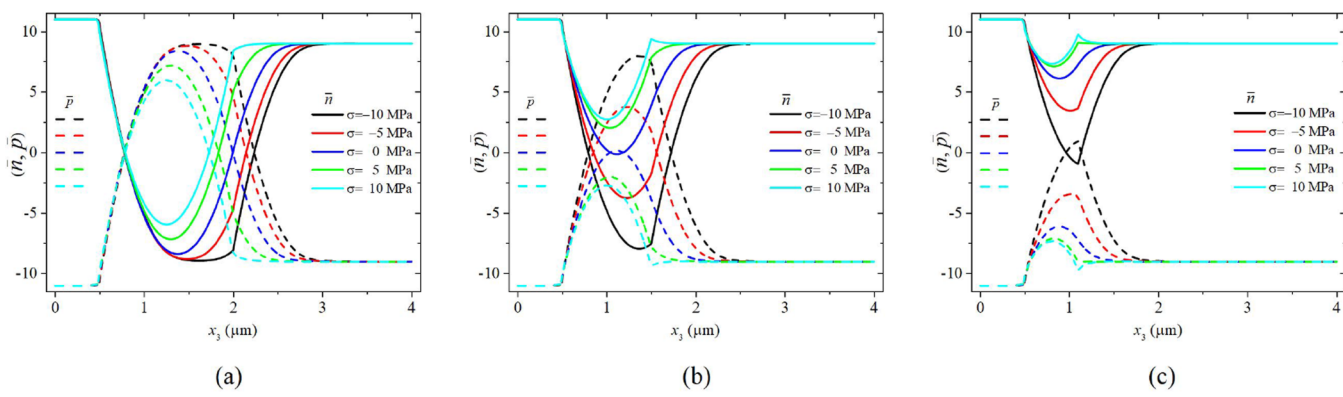


FIG. 3. Carrier concentrations on the AJUT-profile for different base widths under different stresses (a) $d_b = 1.5 \mu\text{m}$, (b) $d_b = 1.0 \mu\text{m}$, and (c) $d_b = 0.6 \mu\text{m}$.

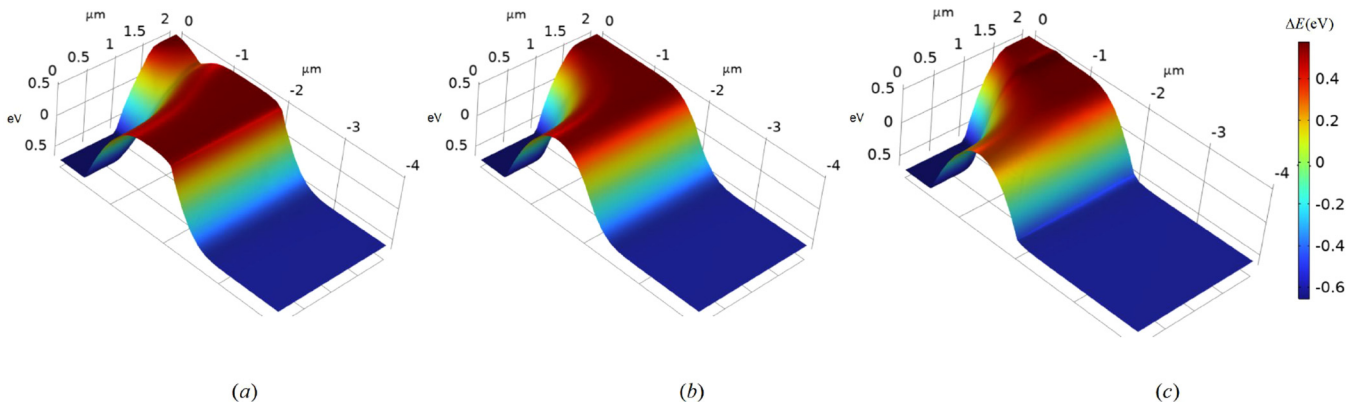


FIG. 4. Energy level difference inside a PS-BJT when σ changing from -10 to 10 MPa (a) $\sigma = -10$ MPa, (b) $\sigma = 0$ MPa, and (c) $\sigma = 10$ MPa.

further elevated such that the electron concentration is always higher than the hole concentration. Thus, it is foreseeable that a pair of great compressive stresses should be applied to induce hole concentration close to electron concentration, which can be found in Fig. 3(c) for $d_b = 0.6 \mu\text{m}$ where the bottom boundary of potential barrier at the B/C junction has reached the E/B interface.

As regards the effect of mechanical loadings on the energy band structure of a PS-BJT, we take a ZnO npn PS-BJT with $d_b = 1.5 \mu\text{m}$ under $(-10, 0, 10)$ MPa as the illustration example. When $\sigma = -10$ MPa acts on the KWZL-plane and MPQN-plane, it follows from Fig. 4(a) that barrier height lowers near the KWZL-plane and rises near MPQN-plane with comparison to the case of $\sigma = 0$ MPa in Fig. 4(b). Difference between electron and hole concentration increases near the KWZL-plane such that the recombination rate in the E/B junction decreases and the corresponding resistivity increases. Obviously, it will produce negative action to the diffusion process of electrons from emitter- to base-region to induce decrease in the number of electrons diffused from the emitter to base region. A decrease in the electron number leads the electron conductivity in the base region to reduce, too. In addition, incremental electric field in the B/C junction reduces by compressive loadings, which will generate weakening in the pumping ability of the B/C junction on electrons. These indicate that compressive loadings produce a negative effect to device performance. Conversely, when $\sigma = 10$ MPa acts on the KWZL-plane and MPQN-plane, it follows from Fig. 4(c) that the barrier height rises near the KWZL-plane and lowers near the MPQN-plane compared to the case of $\sigma = 0$ MPa. Difference between electron and hole concentration decreases near the KWZL-plane such that the recombination rate in the E/B junction increases and the corresponding resistivity decreases. Obviously, it will produce positive action to the diffusion process of electrons from the emitter to base region to induce an increase in the number of electrons diffused from the emitter to base region. Increase in the electron number leads the electron conductivity in the base region to rise, too. In addition, incremental electric field in the B/C junction increases by tensile loadings, which will generate strengthening in the pumping ability

of the B/C junction on electrons. These indicate that tensile loadings produce a positive effect to device performance.

IV. TUNING MECHANISM ON INPUT-, OUTPUT- AND TRANSMISSION-CHARACTERISTICS OF A PS-BJT BY MECHANICAL LOADINGS

A. Influence of base width on the performance of a BJT

The most basic and critical function of a BJT is to lever the large change of collector current I_c through small fluctuation of base current I_b , i.e., the electrons from the emitter region of an npn-type BJT to the base region should be dispatched by base voltage V_{eb} . Thus, the base width cannot be set too large or too small. A too large d_b induces the additional electron-hole recombination after electrons have already gone across the E/B interface, which will reduce the transmission efficiency of the BJT. A too small d_b results in an EP-CE, which causes that part of collector current does not come from the amplification effect of base current. For convenience in the following analysis, three currents (emitter current I_e , base current I_b , and collector current I_c) will be calculated by integral on the three electrodes, respectively,

$$I_e = \int_0^h dx_1 \int_0^{w_e} J_3^n dx_2, I_b = \int_0^h dx_1 \int_0^{w_b} J_3^p dx_2, I_c = \int_0^h dx_1 \int_0^{w_c} J_3^n dx_2. \quad (8)$$

Figure 5 shows dependences of base current I_b upon V_{eb} , collector current I_c upon V_{eb} and dependence of I_c upon I_b of a PS-BJT with base width from 1.00 to $1.30 \mu\text{m}$ under a fixed $V_{ec} = 1.0$ V. Obviously, a narrow base region produces less effect on dependence of I_b upon V_{eb} in Fig. 5(a) (input-characteristics) because almost all holes from base electrode have been driven by V_{eb} to the E/B junction for recombination with electrons and less driven by $(V_{ec} - V_{eb})$ toward the B/C interface. Of course,

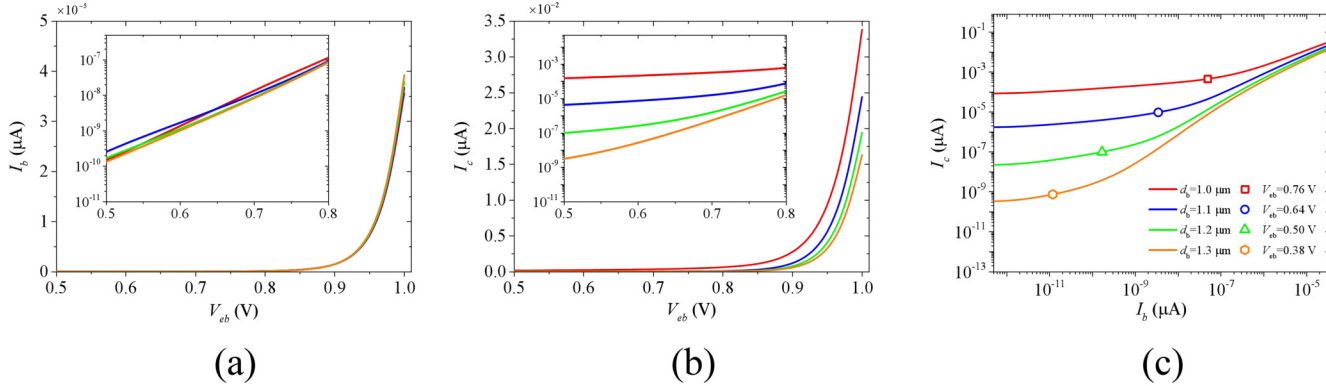


FIG. 5. The input-, output-characteristics and the dependence of I_c upon I_b of a PS-BJT with base width from 1.00 to 1.30 μm under a fixed $V_{ec} = 1.0$ V: (a) $I_b - V_{eb}$, (b) $I_c - V_{eb}$, and (c) $I_c - I_b$.

Downloaded from http://pubs.aip.org/jap/article-pdf/doi/10.1063/5.0141524/jap/168/24/10145701_1_5.0141524.pdf

electron-hole recombination at the E/B junction reduces its resistivity to induce more electrons across the E/B interface such that the base width produces great action on dependence of I_c upon V_{eb} shown in Fig. 5(b). However, the wider the base region is, the more electrons that have already gone across the E/B junction are recombined by holes in the base region outside the E/B junction, which will decrease the transmission efficiency of electrons. In addition, we particularly note that as V_{eb} increases, more holes will be driven to inject from base electrode such that the resistivity at the E/B interface will be further lowered by stronger electron-hole recombination. Moreover, the area of EP-CE on the E/B interface possibly existed in a narrow base region will gradually be extruded and reduced by increasing V_{eb} .

It can be also observed from Fig. 5(b) that a narrower d_b is with a larger I_c because fewer electrons are recombined by holes outside the emitter/base junction. Besides, we also note from Fig. 5(c) that change of I_b is not able to arouse obvious change of I_c when $V_{eb} < V^*$, $V^* = (0.76, 0.64, 0.50, 0.38)$ V for $d_b = (1.0, 1.1, 1.2, 1.3)$ μm . This indicates that an EP-CE exists for a BJT with a narrow d_b when it is subjected to a large $\Delta V_{bc} = V_{ec} - V_{eb}$ such that part of collector current comes from the electron flow through EP-CE. The phenomenon that I_b and I_c are almost independent each other at $V_{eb} < V^*$ implies that the BJT becomes equivalent to two independent diodes: the operating mode of the E/B diode is based on electron-hole recombination, and the one of the B/C diode is based on electron diffusion in EP-CE. Only after $V_{eb} > V^*$, I_c obviously increases with I_b , implying that interaction between the two BJT diodes occurs and the tuning effect of base current on collector current gradually enhances. As V_{eb} further increases from V^* , the current component across EP-CE gradually becomes small compared to the total current I_c and at last can be ignored after V_{eb} becomes enough large. Figure 6 shows the distribution of electron current (white arrow) and hole current (black arrow) in a BJT subjected to $V_{eb} = 0.2$ V and V^* , respectively, with the base width from 1.00 to 1.30 μm under a fixed $V_{ec} = 1.0$ V. When base voltage is relatively small, for example, $V_{eb} = 0.2$ V in the top row of Fig. 6, it is difficult to drive holes by V_{eb} to the whole straight segment LY

(particularly nearby point L) shown in Fig. 1 due to the competition from the collector voltage $V_{ec} = 1.0$ V. Thus, an electronic passageway can be evidently visible near point L for $d_b = 1.0$ and 1.1 μm where almost no holes exist in the EP-CE. The electron current from the emitter region to collector electrode through EP-CE is unaffected by the hole current from the base electrode for a small base voltage, i.e., I_c is almost independent of I_b . When the base voltage increases to arrive at $V_{eb} = V^*$ as shown in the bottom row in Fig. 6, V_{eb} becomes relatively strong to drive holes to more portion of the straight segment LY (particularly nearby point L) such that the electronic passageway has been evidently contracted. Then, most part of electron current flowing toward the collector electrode comes from dispatchment of base voltage V_{eb} .

In order to further study the transmission-characteristics of a BJT, two transmission factors are defined based on the three currents,

$$\nu = I_b/I_e, \beta = I_c/I_b, \quad (9)$$

where ν stands for the proportion of base current I_b to total current I_e and β stands for the current amplification factor of a BJT. We note that ν represents how much information of base current has been adhered to electron current via inter-conversion between majority- and minority-carrier currents inside the E/B junction. Obviously, such an inter-conversion is closely related to the recombination between electrons and holes there. For a narrow d_b with a small V_{eb} , an EP-CE may be induced in the BJT by the potential barrier at the B/C junction, but none EP-CE for a large base width. Thus, there exist three cases for ν when V_{eb} increases from 0 to 1.0 V under V_{ec} fixed as 1.0 V: (1) Regard to a relatively wide base, two regions of emitter and collector have been totally separated without existence of any EP-CE. ν monotonically decreases with increasing V_{eb} , which indicates that the information of base current has been completely adhered on electron current, for example, $d_b = (1.5, 2.0)$ μm ; (2) Regard to a medium width base, an EP-CE exists in the left of the peak and has been completely eliminated at peak by V_{eb} , and none in the right. Thus, ν monotonically increases to peak in the left and monotonically decreases in the right, for

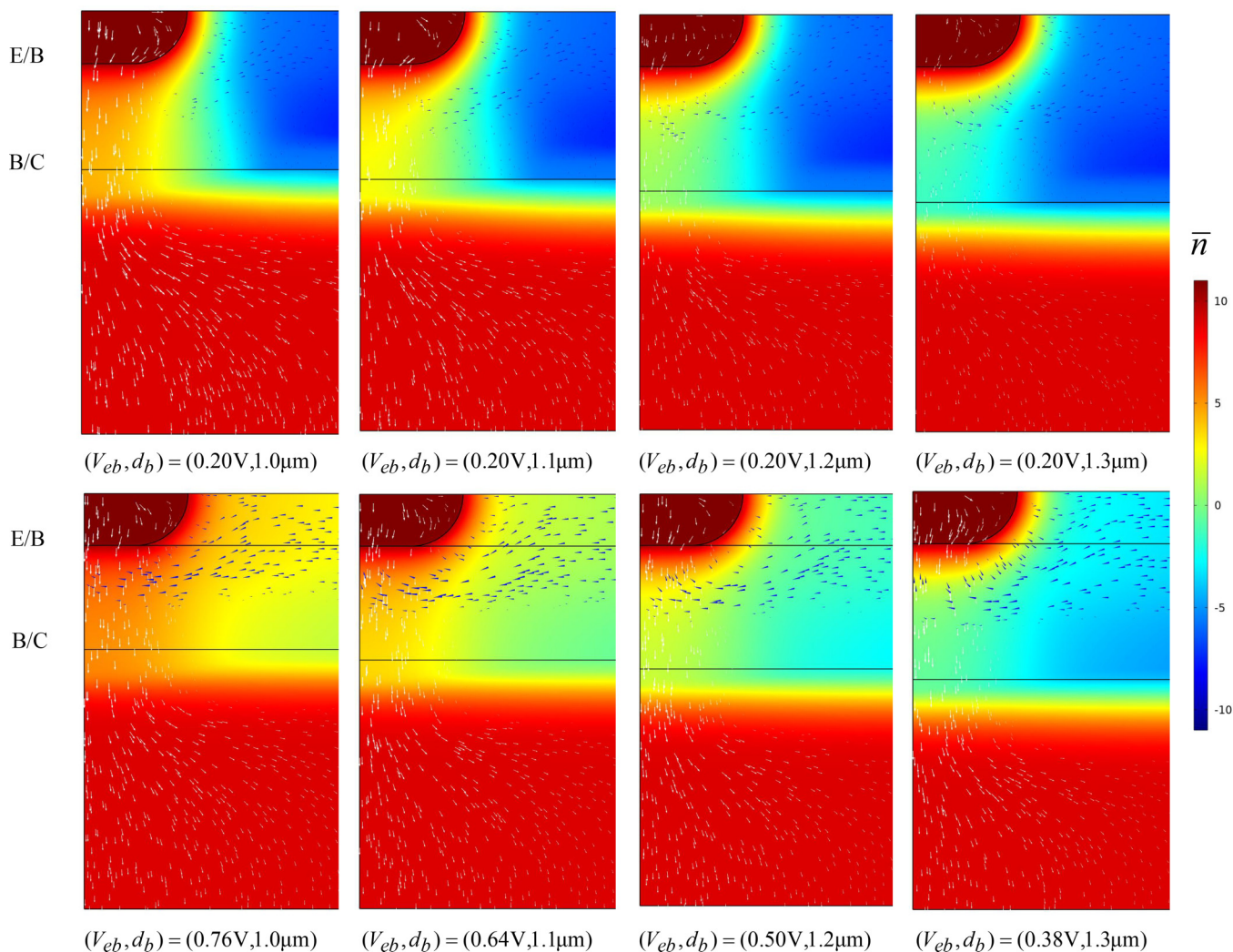


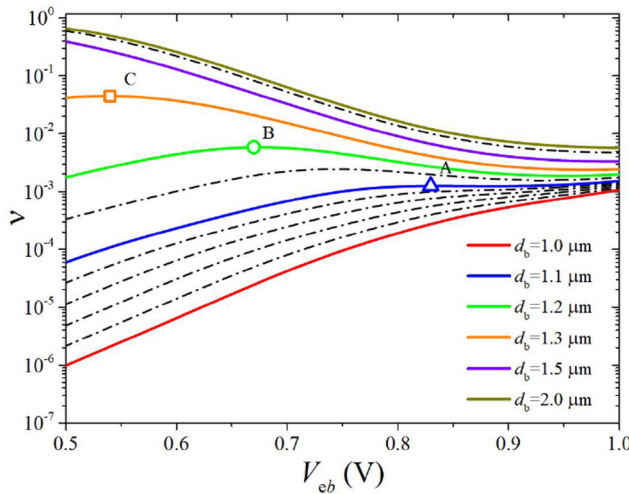
FIG. 6. Distribution of electron current (white arrow) and hole current (black arrow) in the BJT subjected to base voltage $V_{eb} = 0.2$ V and V^* , respectively, with base width from 1.0 to $1.3\mu\text{m}$ under fixed $V_{ec} = 1.0$ V.

Downloaded from http://pubs.aip.org/aip/jap/article-pdf/doi/10.1063/5.0141524/16824610/1_5.0141524.pdf

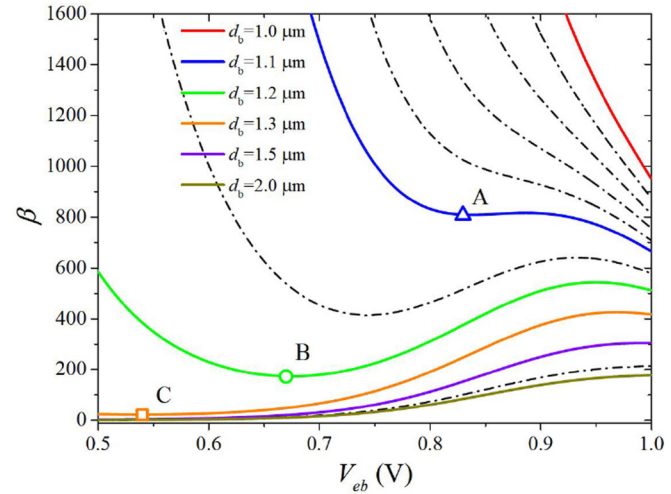
example, at points (A, B, C) for $d_b = (1.1, 1.2, 1.3)\mu\text{m}$. This indicates that I_c on the left side of the peak does not entirely come from the amplification effect of the information of I_b , but the one on the right side does; (3) Regard to an ultrathin base, v always monotonically increases because an EP-CE is always present and just becomes smaller and smaller without totally eliminated by base voltage during V_{eb} increasing from 0 to 1.0 V, for example $d_b = 1.0\mu\text{m}$. Thus, I_c is not entirely from the amplification effect of the information of I_b , that is, as long as there exists an EP-CE, increasing V_{eb} can only induce area enlargement for electron-hole recombination on the emitter interface by extruding the area of EP-CE, but cannot totally eliminate EP-CE area. Thus, we have: (1) For a BJT with a relatively wide base, all the collector current comes from the amplification of base current; (2) For a BJT with a medium wide base such as $d_b = (1.1, 1.2, 1.3)\mu\text{m}$, the collector

current at the left of point (A, B, C) does not completely come from the amplification effect of base current because it also contains the electron current component going through EP-CE, while the collector current at the right of point (A, B, C) does totally come from the amplification effect of base current; (3) For a BJT with a ultrathin narrow base, the collector current does not completely come from the amplification effect of base current because it always contains the current component going through EP-CE.

The above analyses indicate that collector current of a BJT is composed of two parts, one is generated via the amplification effect of base current and the other is generated by the electron flow through EP-CE. The former reflects the amplification information of I_b , while the latter does not. Thus, β defined in (9)₂ is a formal current multiple relationship in fact rather than the real current



(a)



(b)

FIG. 7. (a) Dependence of v upon V_{eb} and (b) Dependence of β upon V_{eb} for a PS-BJT with d_b from 1.00 to 1.30 μm .

Downloaded from http://pubs.aip.org/jap/article-pdf/doi/10.1063/5.0141524/jap/168/24/10145701_1_5.0141524.pdf

amplification factor. According to the base width, useable domain to $\beta \sim V_{eb}$ in the right one of Fig. 7 can be shown as follows: (1) the current amplification factor of a relatively wide BJT is usable in the whole domain for V_{eb} from 0 to 1.0 V; (2) the current amplification factor of a medium wide BJT is usable in the right of the peak v for V_{eb} from V_{peak} to 1.0 V, for example, $V_{peak} = (0.83, 0.67, 0.54)$ V for $d_b = (1.1, 1.2, 1.3)$ μm , respectively; (3) the current amplification factor of an ultrathin BJT is almost un-useable in the whole domain for V_{eb} from 0 to 1.0 V because it always contains the current information from an EP-CE. In order to eliminate the influence of EP-CE on the current amplification factor, it is required to elevate base voltage to extrude and eliminate the area of EP-CE on the emitter/base interface. It follows therefore from Fig. 7(b) that a narrower base region is with a smaller effective operating range of $V_{eb} > V_{peak}$ and even none for too small d_b , for example, $d_b = 1.0 \mu\text{m}$.

B. Tuning mechanism of mechanical loadings on the performance of a PB-BJT

In order to open the sluice gate of electron flow (i.e., E/B interface) as large as possible to drive more electrons across the E/B interface, it is of significance to elevate the electron-hole recombination rate inside the E/B junction to reduce the resistivity. In order to pump more electrons from the base region to the collector region, it is of significance to enlarge the attractive ability of B/C junction with increasing its electron conductivity. As well known in,^{25,26} the resistivity and conductivity of a PN junction with the piezo-effect can be effectively improved via reforming the interface barrier configuration by mechanical loadings, while the attractive ability on electrons of the B/C junction can be promoted by remaking its electric field. In a BJT, the E/B junction is a

forward bias PN junction and the B/C junction is a reversal bias PN junction. For a forward bias junction, the resistivity can be reduced by the mechanical loading mode of driving the majority-carriers from both sides into the junction to enlarge current density going across the junction. For the reversal bias B/C junction, the attractive ability on electrons can be improved by the mechanical loading mode of increasing electric field increment. Thereupon, performance tuning of a PS-BJT is actually to regulate the resistivity of the E/B junction, electric field increment of the B/C junction together with the electron conductivity in base region. Under the c axis set along the x_3 -direction shown in Fig. 1, it follows from Ref. 25 that the loading mode of tensile-stresses can not only drive the majority-carriers into the E/B junction from two sides to elevate its electron-hole recombination rate, but also increase the electric field increment inside the B/C junction and elevate its electron conductivity in the base region. Thus, attention in the following will be paid on the tuning of a pair of tensile stresses applied at the KWZL-plane and MPQN-plane.

Figure 8 shows mechanical tuning on electron current (white arrow) and hole current (black arrow) in the BJT subjected to base voltage $V_{eb} = 0.55$ V with $d_b = 1.5 \mu\text{m}$ under a fixed $V_{ec} = 1.0$ V. A larger σ results in a larger contraction on the size of the potential barrier at the E/B junction with a higher electron-hole recombination rate inside to induce a smaller resistivity $R_e (=dV_{eb}/dI_e)$ as shown in Fig. 9(a). For example, it follows from Fig. 8 that the resistances $R_e (=dV_{eb}/dI_e)$ are $(2.2, 0.99, 0.12) \times 10^{16} \Omega$, respectively, corresponding to $\sigma = (0, 5, 10)$ MPa. Thus, more electrons have been driven across the E/B interface to the base region by mechanical tuning. We also note from Fig. 9(b) that $R_b (=dV_{eb}/dI_b)$ is hardly subjected to the influence of mechanical loadings, i.e., the input characteristics of a PS-BJT are not affected by mechanical regulation, although the output characteristics are greatly affected

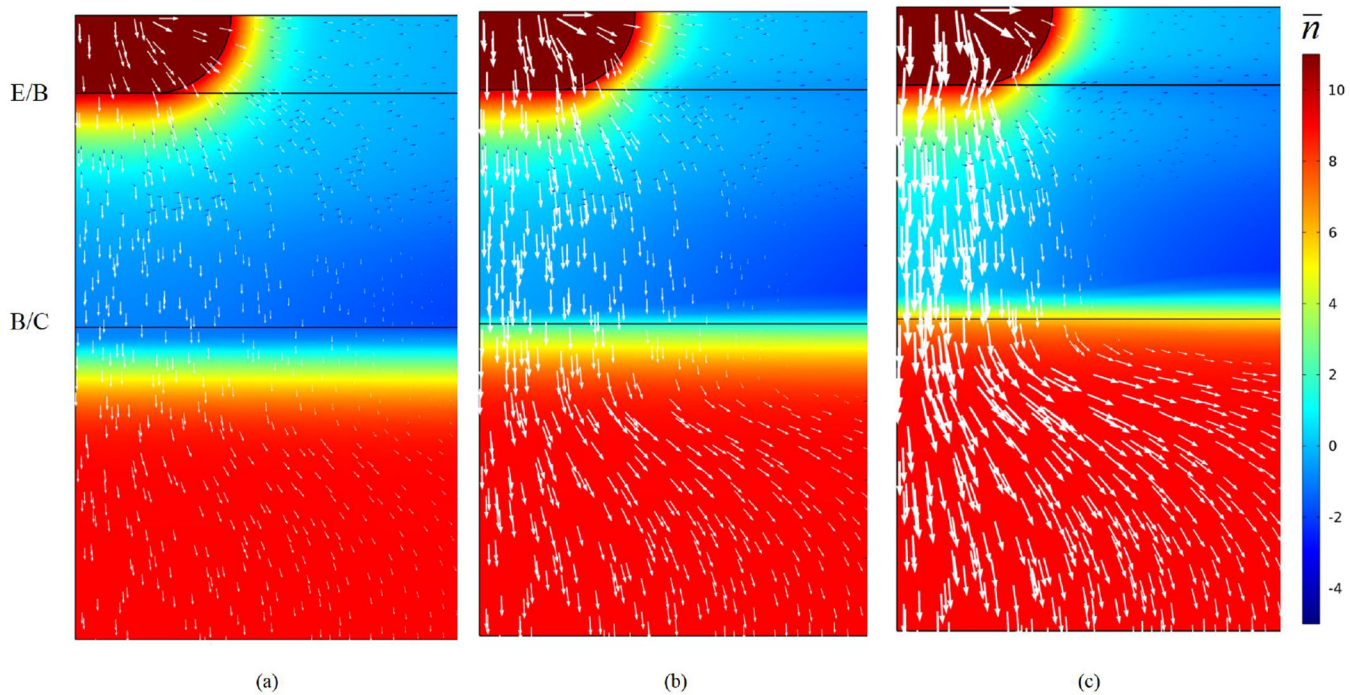


FIG. 8. Mechanical tuning on electron current (white arrow) and hole current (black arrow) in the BJT subjected to base voltage $V_{eb} = 0.55$ V with $d_b = 1.5 \mu\text{m}$ under a fixed $V_{ec} = 1.0$ V: (a) $\sigma = 0$ MPa, (b) $\sigma = 5$ MPa, and (c) $\sigma = 10$ MPa.

Downloaded from http://pubs.aip.org/aip/jap/article-pdf/doi/10.1063/5.0141524/16824610/145701_1_5.0141524.pdf

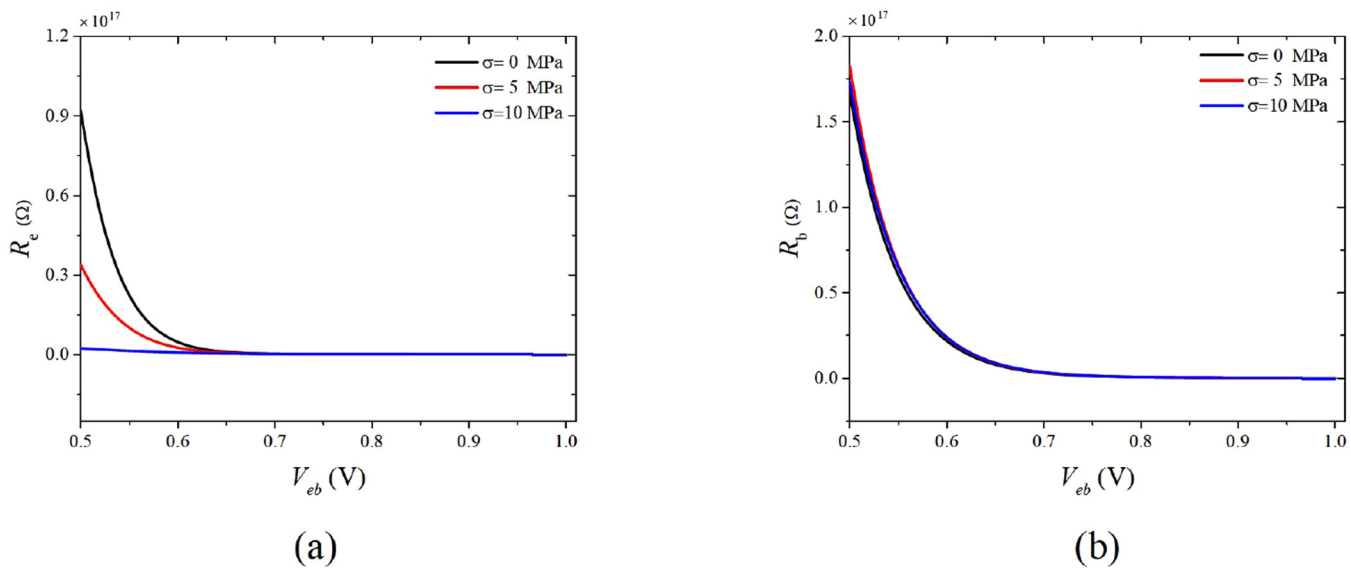


FIG. 9. Dependence of resistivity on V_{eb} of a PS-BJT subjected to different tensile-stress loadings: (a) $R_e - V_{eb}$ and (b) $R_b - V_{eb}$.

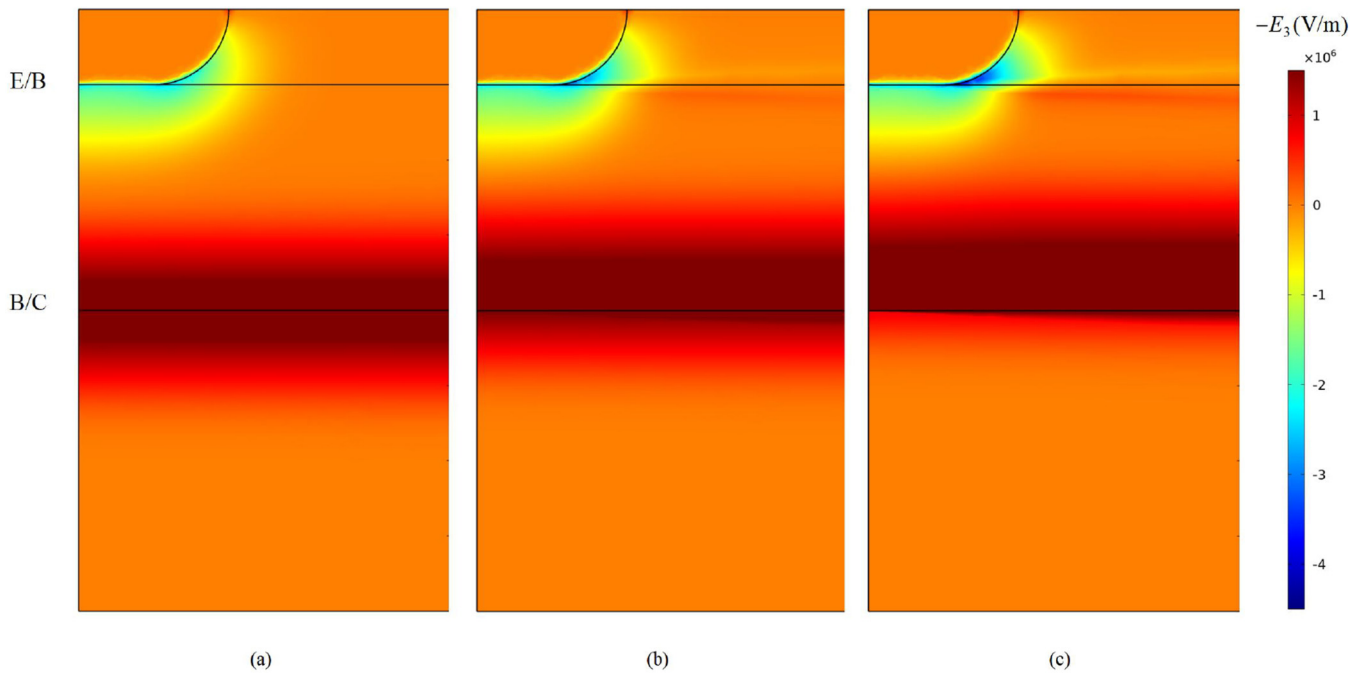


FIG. 10. The component of electric field in the x_3 -direction when a BJT is subjected to $V_{eb} = 0.55$ V with $d_b = 1.5 \mu\text{m}$ under a fixed $V_{ec} = 1.0$ V: (a) $\sigma = 0$ MPa, (b) $\sigma = 5$ MPa, and (c) $\sigma = 10$ MPa.

Downloaded from http://pubs.aip.org/aip/jap/article-pdf/doi/10.1063/5.0141524/16824610/145701_1_50141524.pdf

by mechanical regulation. This is exactly what mechanical regulation on the performance of a PS-BJT requires: to amplify output characteristics as much as possible without causing distortion of input characteristics.

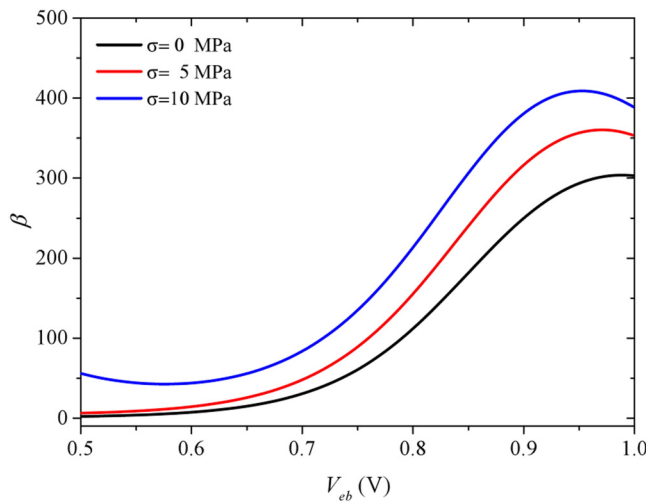


FIG. 11. Dependence of current amplification factor β upon V_{eb} for a PS-BJT with $d_b = 1.5 \mu\text{m}$.

In the same time, we note from Fig. 8 that electron conductivity (directly proportional to electron concentration) in the base region has also been greatly promoted by mechanical tuning. It can be further found from Fig. 10 that in a zone upper the B/C interface, the electric field component in the x_3 -direction has been obviously increased by mechanical loadings, which implies a stronger attractive ability from the B/C junction to the electrons in the base region. It indicates that the stronger attractive ability together with the larger electron conductivity induces more many electrons to be pumped to the collector region as shown in Fig. 8. Thus, the tensile loadings can significantly improve the output current of PS-BJT. For example, when base voltage $V_{eb} = 1.0$ V with $d_b = 1.5 \mu\text{m}$ under a fixed $V_{ec} = 1.0$ V, and the applied stress is taken as $\sigma = (0, 5, 10)$ MPa, $I_c = (1.27, 1.35, 1.43) \times 10^{-2} \mu\text{A}$, respectively.

Figure 11 shows current amplification factor $\beta \sim V_{eb}$ of a PS-BJT with $d_b = 1.5 \mu\text{m}$ under a fixed $V_{ec} = 1.0$ V. Because the mechanical loadings have reduced the resistivity R_e at the E/B junction and aroused the attractive ability of the B/C junction on electrons and the electron conductivity in the base region, the current amplification factor β has been obviously elevated as expected.

V. CONCLUSIONS

Interaction between two junctions in a PS-BJT is analyzed in detail based on establishing a coupling model without the assumption of low injection and depletion layer approximation. It follows from the analyses that the action of the base region in a BJT principally concentrates on the two aspects: one is on the information

transmission from hole current to electron current through the electron-hole recombination in the emitter junction; one is to separate the B/C junction from the E/B junction to prevent the former directly extracting electrons from the emitter region without base regulation. After clarifying the mechanism of mechanical tuning on BJT performance in detail, a mechanical tuning technique is put forward to improve the following issues from the three aspects: (1) reducing the resistivity of the E/B junction to drive more electrons across the E/B interface; (2) elevating the electron conductivity in the base region to ensure an easier pass of electrons; (3) promoting the attractive ability of the B/C junction on the electrons in the base region to pump more electrons across the B/C interface. Numerical results show that the transmission characteristics can be greatly increased as expected by mechanical tuning. Obviously, study on this topic possesses referential significance to mechanical tuning the performance of piezoelectric PN junctions and piezotronic devices.

ACKNOWLEDGMENTS

This work was supported by the National Natural Science Foundation of China (NNSFC) (Grant Nos. 12232007, 11972164, and 12102141) and Chinese Postdoctoral Science Foundation under Grant No. 2022M711252.

AUTHOR DECLARATIONS

Conflict of Interest

The authors have no conflicts to disclose.

Author Contributions

Y.Y. and W.Y. contributed equally to this work.

Yizhan Yang: Data curation (equal); Formal analysis (equal); Software (equal); Visualization (equal); Writing – original draft (equal). **Wanli Yang:** Conceptualization (equal); Funding acquisition (supporting); Investigation (equal); Methodology (equal). **Yunbo Wang:** Conceptualization (equal); Formal analysis (equal); Investigation (equal); Supervision (equal); Validation (equal); Writing – review & editing (equal). **Xiangbin Zeng:** Formal analysis (equal); Investigation (equal); Supervision (equal); Validation (equal); Writing – review & editing (equal). **Yuantai Hu:** Formal analysis (lead); Funding acquisition (lead); Methodology (lead); Project administration (lead); Resources (lead); Supervision (lead); Validation (lead); Writing – review & editing (lead).

DATA AVAILABILITY

The data that support the findings of this study are available from the corresponding author upon reasonable request.

REFERENCES

- ¹G. Zhu, R. S. Yang, S. H. Wang, and Z. L. Wang, “Flexible high-output nanogenerator based on lateral ZnO nanowire array,” *Nano Lett.* **10**, 3151–3155 (2010).
- ²Z. Zhao, Y. Dai, S. X. Dou, and J. Liang, “Flexible nanogenerators for wearable electronic applications based on piezoelectric materials,” *Mater. Today Energy* **20**, 100690 (2021).
- ³Q. Xu, J. Wen, and Y. Qin, “Development and outlook of high output piezoelectric nanogenerators,” *Nano Energy* **86**, 106080 (2021).
- ⁴X. Wang, J. Zhou, J. Song, J. Liu, N. Xu, and Z. L. Wang, “Piezoelectric field effect transistor and nanoforce sensor based on a single ZnO nanowire,” *Nano Lett.* **6**, 2768–2772 (2006).
- ⁵J. Wang, J. F. Jiang, C. C. Zhang, M. Y. Sun, S. W. Han, R. T. Zhang, N. Liang, D. H. Sun, and H. Liu, “Energy-efficient, fully flexible, high-performance tactile sensor based on piezotronic effect: Piezoelectric signal amplified with organic field-effect transistors,” *Nano Energy* **76**, 105050 (2020).
- ⁶P. Zhu, Z. M. Zhao, J. H. Nie, G. W. Hu, L. J. Li, and Y. Zhang, “Ultra-high sensitivity strain sensor based on piezotronic bipolar transistor,” *Nano Energy* **50**, 744–749 (2018).
- ⁷Z. H. Huo, X. D. Wang, Y. F. Zhang, B. S. Wan, W. Q. Wu, J. G. Xi, Z. Yang, G. F. Hu, X. Y. Li, and C. F. Pan, “High-performance Sb-doped p-ZnO NW films for self-powered piezoelectric strain sensors,” *Nano Energy* **73**, 104744 (2020).
- ⁸Z. L. Wang, “Piezopotential gated nanowire devices: Piezotronics and piezophotonics,” *Nano Today* **5**, 540–552 (2010).
- ⁹C. Xie, Y. Wang, Z. X. Zhang, D. Wang, and L. B. Luo, “Graphene/semiconductor hybrid heterostructures for optoelectronic device applications,” *Nano Today* **19**, 41–83 (2018).
- ¹⁰D. L. White, “Amplification of ultrasonic waves in piezoelectric semiconductors,” *J. Appl. Phys.* **33**, 2547–2554 (1962).
- ¹¹A. R. Hutson and D. L. White, “Elastic wave propagation in piezoelectric semiconductors,” *J. Appl. Phys.* **33**, 40–47 (1962).
- ¹²W. Wu, C. Pan, Y. Zhang, X. Wen, and Z. L. Wang, “Piezotronics and piezophotonics—From single nanodevices to array of devices and then to integrated functional system,” *Nano Today* **8**, 619–642 (2013).
- ¹³S. Q. Fan, W. L. Yang, and Y. T. Hu, “Adjustment and control on the fundamental characteristics of a piezoelectric PN junction by mechanical-loading,” *Nano Energy* **52**, 416–421 (2018).
- ¹⁴G. Y. Yang, J. K. Du, J. Wang, and J. S. Yang, “Electromechanical fields in PN junctions with continuously graded doping in piezoelectric semiconductor rods,” *Arch. Appl. Mech.* **92**, 325–333 (2022).
- ¹⁵G. Y. Yang, L. Yang, J. K. Du, J. Wang, and J. S. Yang, “PN junctions with coupling to bending deformation in composite piezoelectric semiconductor fibers,” *Int. J. Mech. Sci.* **173**, 105421 (2020).
- ¹⁶K. Fang, P. Li, N. Li, D. Z. Liu, Z. H. Qian, V. Kolesov, and I. Kuznetsova, “Impact of PN junction inhomogeneity on the piezoelectric fields of acoustic waves in piezo-semiconductive fibers,” *Ultrasonics* **120**, 106660 (2020).
- ¹⁷H. Yildirim, “Excitons in nonpolar ZnO/BeZnO quantum wells: Their binding energy and its dependence on the dimensions of the structures,” *Phys. B* **639**, 413974 (2022).
- ¹⁸N. Liu, M. J. Dan, G. W. Hu, and Y. Zhang, “Piezo-phototronic intersubband terahertz devices based on layer-dependent van der Waals quantum well,” *Nano Energy* **94**, 106912 (2022).
- ¹⁹E. Pan and B. Yang, “Elastic and piezoelectric fields in a substrate AlN due to a buried quantum dot,” *J. Appl. Phys.* **93**, 2435–2439 (2003).
- ²⁰Y. X. Luo, C. L. Zhang, W. Q. Chen, and J. S. Yang, “An analysis of PN junctions in piezoelectric semiconductors,” *J. Appl. Phys.* **122**, 204502 (2017).
- ²¹Z. Yang, L. Sun, C. L. Zhang, C. Z. Zhang, and C. F. Gao, “Analysis of a composite piezoelectric semiconductor cylindrical shell under the thermal loading,” *Mech. Mater.* **164**, 104153 (2022).
- ²²S. Q. Fan, Y. T. Hu, and J. S. Yang, “Stress-induced potential barriers and charge distributions in a piezoelectric semiconductor nanofiber,” *Appl. Math. Mech.* **40**, 591–600 (2019).
- ²³H. Y. Huang, Z. H. Qian, and J. S. Yang, “I-V characteristics of a piezoelectric semiconductor nanofiber under local tensile/compressive stress,” *J. Appl. Phys.* **126**, 164902 (2019).
- ²⁴W. L. Yang, J. X. Liu, Y. L. Xu, and Y. T. Hu, “A full-coupling model of PN junctions based on the global-domain carrier motions with inclusion of the two metal/semiconductor contacts at endpoints,” *Appl. Math. Mech.* **41**, 845–858 (2020).

- ²⁵W. L. Yang, J. X. Liu, and Y. T. Hu, "Mechanical tuning methodology on the barrier configuration near a piezoelectric PN interface and the regulation mechanism on *I-V* characteristics of the junction," *Nano Energy* **81**, 105581 (2021).
- ²⁶Y. Z. Yang, W. L. Yang, Y. B. Wang, X. B. Zeng, and Y. T. Hu, "A mechanically induced artificial potential barrier and its tuning mechanism on performance of piezoelectric PN junctions," *Nano Energy* **92**, 106741 (2022).
- ²⁷S. M. Sze and K. K. Ng, *Physics of Semiconductor Devices* (Wiley-Interscience, 2006).
- ²⁸Z. L. Wang, *Piezotronics and Piezo-Phototronics* (The Science Publishing Company, 2014).
- ²⁹Y. X. Liang and Y. T. Hu, "Effect of interaction among the three time scales on the propagation characteristics of coupled waves in a piezoelectric semiconductor rod," *Nano Energy* **68**, 104345 (2020).